Theor Chim Acta (1991) 78: 241–246

Theoretica
Chimica Acta

On the dynamics of free-radical disproportionation reactions

DeLin Shen and H. O. Pritchard
Chemistry Department, York University, Downsview, Ontario, Canada M3J 1P3

Received February 19, 1990; received in revised form July 10, 1990/Accepted July 13, 1990

Summary. Using *ab initio* potential surfaces, classical (co-planar) trajectory calculations were made for the combination of $H + BeH$ and of $CH + CH$. For the former reaction, disproportionation to $H_2 + Be$ was rare, occurring only for a linear $H \cdots H \cdots Be$ configuration. Likewise, in the second case, the formation of $CH_2 + C$ occurs only via a direct reaction. The principal mechanism in the $CH + CH$ reaction is to form $[C_2H_2]^*$, which dissociates into $C_2H + H$, or very occasionally, directly into $C_2 + H_2$. If the energy is very high, the C_2H radical can dissociate into $C_2 + H$, but sometimes $[C_2H_2]^*$ itself may dissociate simultaneously into $C_2 + H + H$.

Key words: Disproportionation – Recombination – Unimolecular reactions – Trajectory calculations

1. Introduction

The systematisation of the relative rates of disproportionation and combination of pairs of free radicals is a difficult problem [1], made more difficult, in part, by a lack of understanding of the exact mechanism(s) by which these reactions occur. One can find support in the literature for two quite distinct, and mutually exclusive, models of the disproportionation process, e.g.:

$$C_2H_5 + C_2H_5 \rightarrow C_2H_6 + C_2H_4 \tag{1}$$

The more strongly based view is that one radical abstracts a hydrogen atom from the other [2]. The idea received support from early studies, e.g.:

$$CH_3CD_2 + CH_3CD_2 \rightarrow CH_3CHD_2 + CH_2CD_2 \tag{1a}$$

which is isotopically selective in the sense shown [3], from the success of simple geometric models in explaining the variation in combination-disproportionation ratios for simple aliphatic radicals [4], and from the fact that in the case of Eq. (1), there is a secondary minimum in the *ab initio* potential energy surface as one radical approaches the methyl end of the other [5]. An alternative view is that disproportionation is a special case of a chemical activation reaction: in the example above, a $[C_4H_{10}]^*$ complex would be formed, which may then redissociate to two ethyl radicals, it may reorganise its internal motions (as in a unimolecular reaction) and dissociate into ethane and ethylene, or be stabilised by collision to *n*-butane. This view appears to have begun with a tentative discussion by Bradley [6, 7], and has gained gradual acceptance simply as a result of its intrinsic reasonableness: plausible unimolecular reaction treatments of disproportionation reactions, e.g.:

$$HO_2 + HO_2 \rightarrow H_2O_2 + O_2 \qquad (2)$$

have been given [8, 9].

The purpose of the work described here is to examine some recombination processes of simple radicals on *ab initio* potential surfaces that support a second exit channel which may be classed as a disproportionation. The examples chosen were that of:

$$H + BeH \rightarrow Be + H_2 \qquad (3)$$

for which we calculated the surface by standard methods, and of:

$$CH + CH \rightarrow CH_2 + C \qquad (4)$$

on the potential surface calculated previously by Murrell et al. [10, 11].

2. Beryllium hydride recombination reaction

The potential energy surface for BeH_2 was calculated in the 6-311**G Gaussian SCF approximation for approximately 900 combinations of the two BeH bond lengths and the angle between them. In this approximation, BeH exhibits a potential minimum with respect to separated atoms of $-50.14\ \mathrm{kcal\ mol^{-1}}$ at 1.3429 Å (cf. experiment, -49.8 or $-55.8\ \mathrm{kcal\ mol^{-1}}$ and 1.343 Å [12]), and the equilibrium configuration of BeH_2 is linear, bond lengths 1.3321 Å, with an energy of $-124.8\ \mathrm{kcal\ mol^{-1}}$ with respect to separated atoms. Also, in this approximation, the reaction $H + BeH \rightarrow Be + H_2$ is $33\ \mathrm{kcal\ mol^{-1}}$ exothermic: these products are most easily accessible when the H atom approaches H–Be with all three nuclei in a straight line, with a barrier of $2\ \mathrm{kcal\ mol^{-1}}$ if the Be–H bond distance has its equilibrium value; at other angles, the barrier becomes progressively larger as the system becomes more non-linear. In the alternative configuration H–Be···H, the surface is attractive for all H–Be bond lengths provided that the approaching H atom is within 50° of the linear arrangement. There is no low energy path from the H–Be–H arrangement to the H–H–Be one; the least unfavourable path is for the H atom to dissociate from H–Be···H, and re-approach in the opposite orientation. The 6-311**G approximation does not give accurate results at large internuclear distances, so the grid of energy points was confined to those configurations having nearest-neighbour separations of less than 3–3.5 Å. Points for larger distances were interpolated between these and the energy of the appropriate dissociation limit, usually in a Morse-like fashion. The whole grid of points was then fitted to an analytic function by the many-body expansion method used by Murrell's group [13] and a 34-parameter equation with two-body extended Rydberg terms and three-body polynomial terms was able to recover most of the points on the surface to within about $1\ \mathrm{kcal\ mol^{-1}}$.

Trajectory calculations were carried out by standard procedures [14, 15] for various values of the impact parameter, the relative energy of approach between

H and BeH, and of the rotation-vibration energy of the BeH radical; in the latter case, the initial configuration was chosen to be at one of the turning points of the rotating oscillator, these being calculated by the method of Lindberg [16]. The initial rotational motion of the BeH fragment was confined to lie in the plane of the three particles, this being more interesting than rotation perpendicular to the line of centres.

For the most part, the patterns of behaviour are very much as expected. For relative approach velocities $>10^7\ \mathrm{cm\,s^{-1}}$ [$1.09 \times 10^3\ \mathrm{kcal\,mol^{-1}}$] and impact parameters >2.5 Å, the encounter could not be described as a collision. For smaller impact parameters, and for any initial value of J of the BeH fragment, most low-energy collisions ($v_{\mathrm{rel}} < 5 \times 10^4\ \mathrm{cm\,s^{-1}}$ [$2.74 \times 10^{-2}\ \mathrm{kcal\,mol^{-1}}$]) resulted in the formation of an essentially linear H···Be···H complex, the initial angular momentum of the BeH fragment having been converted into overall angular momentum, as suggested by earlier model calculations [17]. The fate of this complex was usually to redissociate into the original fragments, but above $10^7\ \mathrm{cm\,s^{-1}}$, dissociation into 3 fragments was frequent, and below relative approach velocities of $5 \times 10^4\ \mathrm{cm\,s^{-1}}$ exchange often occurred. This exchange usually occurred as a transfer of vibrational energy between the newly formed BeH bond and the original one, but occasionally, through a bending mechanism: for example, we sometimes found a non-linear Be–$H_{(a)}$–$H_{(b)}$ complex with a bond angle of about 140° and having a strong bending motion, which evolved by swinging around so that the $H_{(b)}$ came nearer to the Be atom, after which dissociation into $BeH_{(b)}$ and $H_{(a)}$ took place.

Our main interest was in the formation of $Be + H_2$, which could only occur for relative approach energies $>2\ \mathrm{kcal\,mol^{-1}}$ [$\sim 5 \times 10^5\ \mathrm{cm\,s^{-1}}$]. However, it was found to occur only in the case of an *identically* head-on configuration; the existence of a slightly non-zero impact parameter, or of any rotational motion of the BeH fragment allowed the complex to achieve the H–Be–H configuration, which would never eliminate H_2. In most cases, this occurred via a compound collision in which the incident H atom, having imparted some rotational motion to the H–Be fragment, was captured by the Be atom before it had recoiled out of range (see e.g. Fig. 4 of [17]). Thus, disproportionation on this surface is an infinitesimally rare event, occurring through a direct head-on abstraction by the attacking hydrogen; we did not find a single example where it occurred via a unimolecular decomposition of a H–Be–H complex.

3. Acetylene recombination reaction

This somewhat surprising result led us to examine another, and more realistic, disproportionation reaction, Eq. (4). We used the co-planar many-body ground-state potential calculated by Murrell et al. [10, 11], later modified to be valid at all dissociation limits as well as in the regions close to equilibrium [11]. Relative to the energy of the two separated $CH(X, {}^2\Pi)$ radicals, this potential exhibits a minimum at $-236.5\ \mathrm{kcal\,mol^{-1}}$, with exit channels to $CH_2(\tilde{X}, {}^3B_1) + C({}^3P)$ at $-23.6\ \mathrm{kcal\,mol^{-1}}$ and to $C_2H(\tilde{X}, {}^2\Sigma^+) + H({}^2S)$ at $-111.0\ \mathrm{kcal\,mol^{-1}}$. Technically, both of these exit channels are disproportionations, but only the first one is of interest to us here, as being representative of the kind of process depicted in Eq. (1). On this surface, the minimum for the vinylidene structure lies at $-196.5\ \mathrm{kcal\,mol^{-1}}$, with the transition configuration for isomerisation to acetylene being at -187.9 kcal mol^{-1}. The formation of $C_2(X, {}^1\Sigma_g^+) + 2H({}^2S)$ is also possible at $+23.6$ kcal mol^{-1} above the energy of 2CH.

Over a wide range of approach energies and impact parameters, it was found that a $[C_2H_2]^*$ configuration in which the two C atoms and one H atom formed an approximately equilateral triangle was a common occurrence. We found that disproportionation into $CH_2 + C$, i.e. the analogue of Eq. (1), only occurred for a very restricted set of initial conditions: the initial orientation had to be H–C···H–C, with little or no rotation, with an impact parameter of <0.075 Å at a relative approach velocity of 10^4 cm s^{-1}; the higher the relative velocity, the smaller was the impact parameter for which this reaction would occur. Just outside this "cone of acceptance", i.e. slightly too large an impact parameter or relative velocity, the system was able to slide round and achieve the common triangular C–C–H configuration, after which the trajectory behaved like those of other normal collision events.

The usual behaviour below the $C_2 + 2H$ threshold, regardless of the initial velocity or degree of rotational or vibrational excitation, was to form a $[C_2H_2]^*$ complex, either triangular or essentially linear H···C···C···H, which sometimes would redissociate to 2CH, but more usually into $C_2H + H$, within a period of approximately 1.5×10^{-12} s. Above the $C_2 + 2H$ threshold, dissociation into $C_2H + H$ took place in some $2\text{–}3 \times 10^{-13}$ s, with subsequent dissociation into $C_2 + H$ within a further 4×10^{-13} s.[1]

We encountered one remarkable trajectory, which is shown in Fig. 1, as it illustrates, also, many of the features of the recombination process: in this encounter, there was a direct reaction:

$$CH + CH \rightarrow C_2 + H_2 \tag{6}$$

which is exothermic by 85.9 kcal mol^{-1}, but it did not occur through the traditional "four-centre transition state". There are six internuclear distances, which are depicted in pairs in three panels of the diagram. In this collision, one CH radical ($C_{(a)}$–$H_{(b)}$) was in $v = 7$, $J = 0$, and the other ($C_{(c)}$–$H_{(d)}$) in $v = 0$, $J = 1$, with an impact parameter of 0.081 Å, a relative approach velocity of 10^4 cm s^{-1} and the carbon end of the rotationless radical pointing towards the centre of mass of the other one. Panel [1] shows the separations of $C_{(a)}$ from $H_{(b)}$ and $H_{(d)}$: the strong undulation in the $C_{(a)}$–$H_{(d)}$ distance is due to the rotation of $C_{(c)}$–$H_{(d)}$ about its own centre of mass near $C_{(c)}$, but this rotation is annihilated by the time the internuclear separations are between 4 and 5 Å, with its angular momentum going into overall angular momentum. Panel [3] shows the separations of $H_{(d)}$ from $H_{(b)}$ and $C_{(c)}$: the amplitude of the $C_{(c)}$–$H_{(d)}$ vibration is much less than that of the $C_{(a)}$–$H_{(b)}$ vibration in Panel [1], but the $H_{(b)}$–$H_{(d)}$ separation shows the same undulation as does the $C_{(a)}$–$H_{(d)}$ distance, due to $C_{(c)}$–$H_{(d)}$ rotation. After the encounter, at about 1.6×10^{-12} s, the strong

---

[1] Very little is known about the reaction between two CH radicals, and where they occur in a system, are usually assumed to form acetylene [18, 19]. Our observations would indicate that the rate of the reaction:

$$CH + CH \rightarrow C_2 + 2H \tag{5}$$

could have a frequency factor close to the collision number, and an Arrhenius temperature coefficient close to the endothermicity; also, the unimolecular decompositions of $[C_2H_2]^*$ into $C_2H + H$ and of C_2H into $C_2 + H$, which are ignored, may play an important role, especially so at low pressures

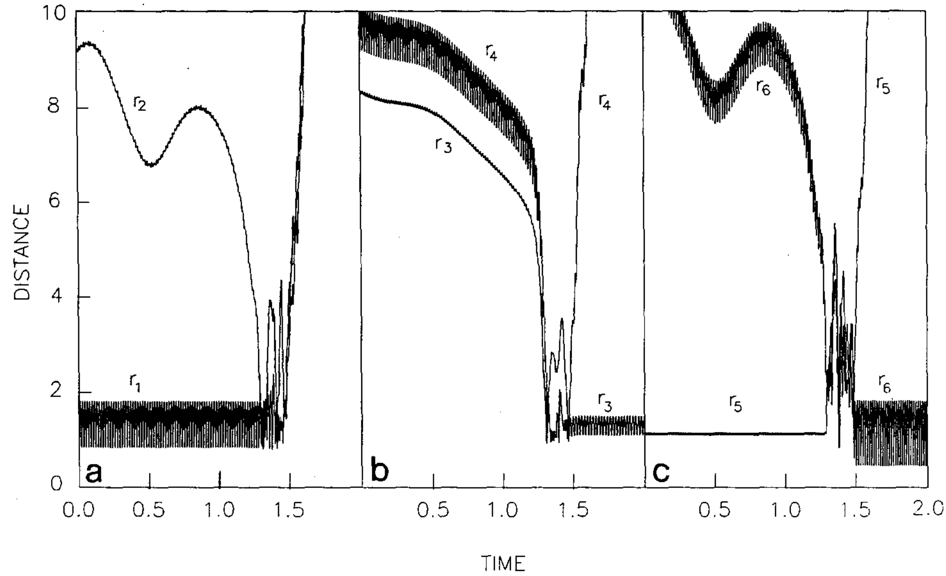

Fig. 1. Behaviour of the six internuclear distances in the process $2CH \rightarrow C_2 + H_2$, as described in the text: **a** $r_1 = C_{(a)}\text{–}H_{(b)}$, $r_2 = C_{(a)}\text{–}H_{(d)}$; **b** $r_3 = C_{(a)}\text{–}C_{(c)}$, $r_4 = C_{(c)}\text{–}H_{(b)}$; **c** $r_5 = C_{(c)}\text{–}H_{(d)}$, $r_6 = H_{(b)}\text{–}H_{(d)}$. Distances are in Å and times in units of 10^{-12} s. (Note: the patterning of the traces of r_1, r_4 and r_6 is an artefact due to rounding of the dot coordinates in the laser printer)

oscillation of the resultant H_2 is seen ($v \sim 8$, $J \sim 6$). Panel [2] shows the separations of $C_{(c)}$ from $C_{(a)}$ and $H_{(b)}$, and it is seen that the product C_2 (in $v \sim 6$, $J \sim 31$) is well established at about the same time; conservation of angular momentum is assured by the fact that the relative recoil velocity is now about 6×10^5 cm s^{-1}, with an asymptotic offset between the two paths of around 2.2 Å. During the period from 1.3 to 1.6×10^{-12} s, the lifetime of the $[C_2H_2]^*$ complex, the predominant geometry is a triangular one (and not the expected four-centre configuration).

4. Conclusions

From the standpoint of understanding the disproportionation process (1), calculations on these triatomic and tetratomic surfaces can only offer a very limited insight. In particular, for such small systems, the lifetime of any complex with respect to unimolecular decay is very short, so that chemical activation pathways[2] are automatically discriminated against with respect to alternative abstrac-

---

[2] Also, the real process (4) to give $CH_2 + C$ is complicated by the existence of another surface which can lead to singlet CH_2 radicals at very nearly the same energies; however, since our principal interest is in the general disproportionation process (1) rather than in the specific reaction (4), we did not consider this surface to be relevant. A second complication with this surface which, to some extent, affects the generality of the results is the existence of an energetically favourable exit channel below the one of interest, which is absent in Eq. (1)

tion processes. Our interim results, therefore, can only be taken as an indication of the need for further work.

In our two sets of trajectory studies, the disproportionation process in which both H atoms end up bonded to the same centre appears only to occur as a direct abstraction reaction. Other related calculations have been performed by Harding and Wagner: in one, the reaction [20]:

$$HO + HO \rightarrow H_2O + O \tag{7}$$

appears to be a direct process, with no involvement of the $[H_2O_2]^*$ species, and in the other [21]:

$$H + CHO \rightarrow H_2 + CO \tag{8}$$

direct abstraction is an order of magnitude faster at low temperature than is the scrambling reaction. Also, there is firm experimental evidence that H_2 is not formed in the disproportionation of two HO_2 radicals [22]. Thus, until it is possible to classify disproportionation reactions as to whether they are to be regarded as abstraction or chemical activation processes, unimolecular reaction treatments of disproportionation reactions should be viewed with some caution.

Acknowledgements. This work was made possible by support from the Natural Sciences and Engineering Research Council of Canada; we are also indebted to Dr A. C. Hopkinson for his assistance in performing the Gaussian calculations.

References

1. Nilsson WB, Pritchard GO (1982) Int J Chem Kinetics 14:299–323
2. Kerr JA, Trotman-Dickenson AF (1961) Prog Reaction Kinetics 1:105–127
3. Wijnen MHJ, Steacie EWR (1951) Can J Chem 29:1092–1103
4. Benson SW (1983) Can J Chem 61:881–887
5. Minato T, Yamabe S, Fujimoto H, Fukui K (1978) Bull Chem Soc Japan 51:1–10
6. Bradley JN (1961) J Chem Phys 35:748–750
7. Bradley JN, Rabinovitch BS (1962) J Chem Phys 36:3498–3499
8. Pilling MJ, Smith IWM (1987) Modern gas kinetics. Blackwell Oxford, pp 210–213
9. Walker RW (1988) Twenty Second Symposium (International) on Combustion, The Combustion Institute, Pittsburgh, pp 883–892
10. Carter S, Mills IM, Murrell JN (1980) Mol Phys 41:191–203
11. Halonen L, Carter S, Child MS (1982) Mol Phys 47:1097–1112
12. Pople JA, Frisch MJ, Luke BT (1983) Int J Quantum Chem (Supplement) 17:307–320
13. Murrell JN, Carter S, Farantos SC, Huxley P, Varandas AJC (1984) Molecular potential energy functions. Wiley, New York
14. Miller WH (1974) Adv Chem Phys 25:69–177
15. Bunker DL (1971) Methods Comp Phys 10:287–325
16. Lindberg B (1988) J Chem Phys 88:3805–3810
17. Cohen LK, Pritchard HO (1985) Can J Chem 63:2374–2377
18. Braun W, Welge KH, McNesby JR (1966) J Chem Phys 45:2650–2658
19. Spangenberg HJ, Börger I, Drost H, Klotz HD (1986) Zeit phys Chem (Leipzig) 267:1081–1097
20. Harding LB, Wagner AF (1988) Twenty Second Symposium (International) on Combustion, The Combustion Institute, Pittsburgh, pp 983–989
21. Harding LB, Wagner AF (1986) Twenty First Symposium (International) on Combustion, The Combustion Institute, Pittsburgh, pp 721–728
22. Stephens SL, Birks JW, Glinski RJ (1989) J Phys Chem 93:8384–8385